Check for updates

International Journal of Energy Research

WILEY

RESEARCH ARTICLE OPEN ACCESS

Ethanol-Based Biodiesel Production From Cottonseed Oil via Water-Tolerant Thermally Induced Noncatalytic Transesterification

Gyeongnam Park[1] | Jung-Hun Kim[1] | Minyoung Kim[1] | Jee Young Kim[2] | Doyeon Lee[3] | Eilhann E. Kwon[1]

[1]Department of Earth Resources and Environmental Engineering, Hanyang University, Seoul 04763, Republic of Korea | [2]Department of Environmental and Safety Engineering, Ajou University, Suwon 16499, Republic of Korea | [3]Department of Civil and Environmental Engineering, Hanbat National University, Daejeon 34158, Republic of Korea

Correspondence: Doyeon Lee (dylee82@hanbat.ac.kr) | Eilhann E. Kwon (ek2148@hanyang.ac.kr)

Received: 6 May 2026 | **Revised:** 31 August 2026 | **Accepted:** 13 October 2026

ABSTRACT

Biodiesel is a renewable fuel that replaces petro-diesel in the transportation sector and supports efforts to resolve anthropogenic global warming. However, the use of methanol in biodiesel production lowers its sustainability because methanol is being produced from natural gas. The use of biomass-derived ethanol in biodiesel production offers a more sustainable basis. Despite the environmental advantages of ethanol, its residual water content limits its practical application in conventional base-catalyzed processes. This study proposes a thermally induced noncatalytic process for ethanol-based biodiesel production. In this process, thermal energy induces the cleavage of ester bonds in triglycerides, generating fatty acid intermediates that subsequently react with ethanol to form fatty acid ethyl esters (FAEEs). Meanwhile, the confinement effect provided by a porous material enhances interfacial contact between the immiscible reactants and accelerates the reaction without externally applied pressure. Cottonseed (23.8 wt.% of oil content) was used as a biodiesel feedstock. Due to the steric hindrance caused by ethanol's larger molecular size, conventional base-catalyzed transesterification yielded 14.2 wt.% biodiesel at 70°C for 120 min. In contrast, thermally induced noncatalytic transesterification produced up to 88.1 wt.% biodiesel at 380°C in 1 min. With increasing water content, the FAEE yield decreased to 76.9 wt.% at 10 wt.% water, while a relatively high yield of 85.4 wt.% was maintained at 4 wt.% water, corresponding to 96 wt.% ethanol. These results suggest the potential of utilizing water-containing ethanol as the alcohol feedstock for transesterification. Moreover, the use of FAEE produced through the noncatalytic transesterification of cottonseed oil was estimated to mitigate carbon dioxide (CO_2) emissions by 1.16 g g_{seed}^{-1}. Accordingly, the application of thermally induced noncatalytic process for ethanol-based biodiesel production would strengthen the shift toward sustainable transport systems.

1 | Introduction

It is indisputable that rising atmospheric concentration of carbon dioxide (CO_2) is closely linked to increasing global temperatures, driving the progression of global warming [1]. To avert the escalating frequency and intensity of climate-induced natural disasters, reducing anthropogenic carbon emissions has become an urgent priority [2]. Achieving this requires an identification of carbon-emitting sectors, followed by the deployment of technologies capable of reducing emissions where such mitigation is feasible. Given that the use of diesel in the transportation sector forms the second-largest source of human-driven CO_2 emissions [3], emission reduction in this sector makes an effective contribution to the effort to address global warming. As such, biodiesel production from biomass-derived oils have gained attention due to their intrinsic carbon neutrality and seamless compatibility with existing fuel distribution infrastructure [4, 5].

This is an open access article under the terms of the Creative Commons Attribution License, which permits use, distribution and reproduction in any medium, provided the original work is properly cited.

Copyright © 2026 Gyeongnam Park et al. *International Journal of Energy Research* published by John Wiley & Sons Ltd.

Biodiesel is synthesized through transesterification, a reaction in which oils (triglycerides) react with primary alcohols to form fatty acid alkyl esters [6]. Homogeneous base catalysts such as potassium hydroxide (KOH) cleave the ester bonds in triglycerides, and the released fatty acids then react with alcohol molecule [7]. Methanol is used to commercially convert oils to fatty acid methyl esters (FAMEs) because it offers high reactivity and low cost [8]. While the use of methanol is the current standard for biodiesel production, methanol is obtained from fossil fuel (natural gas), which results in carbon emissions during its manufacture [9]. This creates an ironic situation in which the production and use of biodiesel for CO_2 reduction are constrained by the carbon released in the upstream process. In addition, because methanol is a toxic chemical, the process requires multiple safety measures and additional operational controls, and regulatory management [10].

As an alternative alcohol, ethanol has gained considerable attention due to its lower toxicity and higher sustainability than methanol [11]. Ethanol production from biomass provides a nonfossil route for biodiesel synthesis [12]. Biodiesel produced with ethanol, known as fatty acid ethyl esters (FAEEs), exhibits enhanced fuel properties compared to FAMEs, including higher cetane number, greater calorific value, and improved cold flow performance [13]. Despite these advantages of FAEEs, the use of ethanol in biodiesel production presents technical challenges. Because the base catalyst used in transesterification is susceptible to impurities (nonlipid components) [14], high purity of oils and ethanol are required to ensure a biodiesel yield. However, ethanol produced from biomass has low purity (≤96%) because it contains water [12]. The separation of an azeotropic mixture such as water and ethanol through distillation is limited [15]. Water induces hydrolysis of triglycerides, forming free fatty acids (FFAs) [16]. FFAs readily react with base catalysts to form soap via saponification, reducing the biodiesel yield and complicating product separation [17]. Therefore, technical progress is needed to enable efficient production of ethanol-based biodiesel (FAEEs).

To overcome the limitations of conventional base-catalyzed transesterification, noncatalytic transesterification under supercritical ethanol conditions has been developed. However, systematic evaluations of the process tolerance toward water-containing ethanol remain limited [18–20]. Moreover, the need to apply high external pressure (>30 MPa) increases operating costs and raises process safety concerns [21]. Therefore, this study proposes a thermally induced noncatalytic transesterification process that can operate without external pressurization. The proposed process is driven by thermal energy, which initiates transesterification through the cleavage of ester bonds in triglycerides without the use of water-sensitive catalysts. In addition, a porous material was introduced to provide a confinement effect that enhances reactant collision frequency, thereby promoting transesterification. Accordingly, this study aims to investigate the potential of thermally induced noncatalytic transesterification using water-containing ethanol and to assess its potential for sustainable biodiesel production. Cottonseed is a major byproduct of the cotton fiber industry [22]. It contains 11%–25% oils, which is comparable to the oil content of soybeans (15%–20%), a representative feedstock for commercial biodiesel production [23, 24]. Given its high oil content, cottonseed was used in this study to extract oils for use as feedstock in biodiesel production. Such an effort promotes waste valorization in the cotton fiber industry and contributes to sustainable biodiesel production. The objectives of this study are threefold: (i) to compare the FAEE yield obtained using the proposed noncatalytic approach with that from conventional base-catalyzed transesterification, (ii) to optimize the reaction temperature for synthesizing FAEEs from cottonseed oil via noncatalytic transesterification, and (iii) to evaluate the influence of water and FFAs on FAEE yield in noncatalytic transesterification.

2 | Materials and Methods

2.1 | Chemical Reagents

Silica (SiO_2; 6 nm mean pore size, 480 $m^2 g^{-1}$ specific surface area, 0.75 $cm^3 g^{-1}$ pore volume, Prod. No. 236799), nonporous silica (SiO_2; 300 nm particle size, Prod. No. 904422), barium hydroxide ($Ba(OH)_2$; 95.0%, Prod. No. 433373), phenolphthalein ($C_{20}H_{14}O_4$; 0.5 wt.% in ethanol:water (1:1), Prod. No. 319236), FAME standard mixture (Prod. No. CRM47885), and FAEE standard mixture (Prod. No. 49454-U) were purchased from Sigma–Aldrich, USA. Dichloromethane (DCM; CH_2Cl_2; ≥99.8%, Prod. No. 3030-2304), methanol (CH_3OH; ≥99.9%, Prod. No. 5558-2304), ethanol (C_2H_5OH; ≥99.9%, Prod. No. 4023-4100), n-hexane (C_6H_{14}; ≥95.0%, Prod. No. 4081-4410), and iso-propanol (C_3H_8O; ≥ 99.5%, Prod. No. 5035-4410) were obtained from DAEJUNG Chemicals, Korea. KOH (95.0%, Prod. No. P1422) and toluene (C_7H_8; ≥99.5%, Prod. No. 000T0497) were purchased from SAMCHUN Chemicals, Korea. Linoleic acid ($C_{18}H_{32}O_2$; 99.0%, Prod. No. 215040050) was purchased from Thermo Fisher scientific, USA.

2.2 | Cottonseed Oil Extraction

Cottonseeds were supplied from a local farm in Korea and dried in a convection oven at 105°C for 24 h to remove moisture and milled for oil extraction. Cottonseed oil was obtained from Soxhlet extraction with 70.0 ± 0.5 g of cottonseeds and 800 mL of n-hexane. Extraction was done at 90°C for 48 h. Solvent was then evaporated by a rotary evaporator (WiseVaporTM Ev-1001 V, SciLab, Korea) to recover extract (crude cottonseed oil). The FFA content in crude cottonseed oil was determined by measuring acid value (AV) according to ASTM D974-12. 100 mL of titration solution (toluene, water, and iso-propanol in a volumetric ratio 100:1:99) was mixed with 2.0 ± 0.1 g of cottonseed oil, followed by the addition of phenolphthalein (0.5 mL) as a color indicator. The mixture was titrated with a 0.1 M KOH solution until a color change was observed, and the AV (mg KOH g^{-1}oil) was calculated based on the volume of titrant consumed.

2.3 | Thermogravimetric Analysis (TGA)

TGA was performed using a STA 449 F5 Jupiter (NETZSCH, Germany). 10 ± 0.1 mg of cottonseed, cottonseed oil, or refined soybean oil was placed in an alumina crucible. TGA tests were carried out over a temperature range of 40–900°C at a heating rate of 10°C min^{-1}. Nitrogen (N_2) was employed as the purge and protective gas, with flow rates of 80 and 20 mL min^{-1},

ijer, 2026, 1, Downloaded from https://onlinelibrary.wiley.com/doi/10.1155/er/8176983 by Hanyang University Library, Wiley Online Library on [16/11/2026]. See the Terms and Conditions (https://onlinelibrary.wiley.com/terms-and-conditions) on Wiley Online Library for rules of use; OA articles are governed by the applicable Creative Commons License

respectively. To correct for mass changes caused by gas buoyancy effect, blank tests with an empty crucible were conducted under the same operating conditions prior to sample analysis.

2.4 | Biodiesel Production

2.4.1 | Base-Catalyzed Transesterification

Base-catalyzed transesterification of cottonseed oil (5.0 ± 0.1 g) was performed using 1.5 wt.% of KOH (based on oil mass) and an alcohol-to-oil molar ratio of 6:1 using either methanol or ethanol as alcohol. In addition to the 6:1 condition, ethanol-based transesterification was further conducted at an increased alcohol-to-oil molar ratio of 12:1 to examine the effect of increased ethanol loading on FAEE yield. To prepare a homogeneous catalyst solution, KOH was dissolved in the respective alcohol and stirred for 10 min at 400 rpm. KOH–alcohol mixture was then added to the cottonseed oil and reacted at 60°C for 120 min with methanol and 70°C for 120 min with ethanol. After the reaction, the products were separated into biodiesel and glycerol layers using a separating funnel. Biodiesel was then diluted with DCM and subjected to quantitative and qualitative analyses using gas chromatography with a flame ionization detector (GC/FID; 8890, Agilent, USA) and GC/mass spectrometry (GC/MS; 5977 B, Agilent, USA), respectively. The detailed operating parameters for GC/FID and GC/MS are summarized in Tables S1 and S2. The biodiesel components were identified by GC/MS using the National Institute of Standards and Technology (NIST) mass spectral library. The concentration of each ester was determined from its corresponding GC peak area using the calibration curve, and the biodiesel yield was calculated according to the following equation:

$$\text{Biodiesel yield (wt.\%)} = \frac{A \times \text{RF} \times V_{\text{d}}}{W_{\text{oil}}} \times 100,$$

where A is the GC peak area of FAME or FAEE, RF is the response factor ($\mu g\,mL^{-1}$ peak $area^{-1}$) obtained from the calibration curve, V_{d} is the dilution volume (mL), and W_{oil} is the initial mass of cottonseed oil (μg). The calibration data are provided in Tables S3 and S4, while the detailed calibration information, including response factors, linear ranges, and detection limits, is summarized in Tables S5 and S6.

2.4.2 | Noncatalytic Transesterification

For the noncatalytic transesterification of cottonseed oil, a 1 mL batch reactor was assembled with a bulkhead union (SS-400-61, Swagelok, USA) and two stoppers (SS-400-P, Swagelok, USA). The reactor was filled with 7.5 ± 0.1 mg (≈8.2 μL) of cottonseed oil and 320.0 ± 0.5 mg of silica. Methanol and ethanol were added at volumes of 200 and 289 μL, respectively, corresponding to an alcohol-to-oil molar ratio of 568:1 for both reaction systems. Thermally induced noncatalytic transesterification was conducted in a 1 mL batch reactor over a temperature range of 250–390°C without externally applied pressure. The autogenous pressure under the reaction conditions was estimated using the Peng–Robinson equation [25], with the detailed calculation procedure provided in the Supporting Information. The parameters used and the estimated pressures are summarized in Table S7. To investigate the relative reactivity of ethanol compared to methanol, mixed alcohols with methanol-to-ethanol molar ratios of 1:3, 2:2, and 3:1 were also prepared, with corresponding volumes used in the noncatalytic reaction were 267, 245, and 222 μL, respectively. In addition, the tolerance of the thermally induced noncatalytic reaction to water and FFAs was evaluated. For the water-content experiments, ethanol/water mixtures containing 2, 4, 6, 8, and 10 wt.% water were prepared. The volume of ethanol was fixed at 289 μL, corresponding to 228.0 mg based on an ethanol density of $0.789\,g\,mL^{-1}$ [26]. Accordingly, 4.7, 9.5, 14.6, 19.8, and 25.3 mg of water were added to obtain water contents of 2, 4, 6, 8, and 10 wt.%, respectively. The corresponding water volumes were calculated using a water density of $0.998\,g\,mL^{-1}$ [27], and ethanol and water were premixed before being introduced into the reactor. For the FFA-addition experiments, FFAs were added at 2, 4, 6, 8, and 10 wt.% relative to the mass of cottonseed oil. The mass of cottonseed oil was fixed at 7.5 mg in all experiments. These investigations were conducted at 380°C. After reaching the target temperature, the reactor was removed from the furnace within 1 min and cooled to 20°C. Accordingly, the effective residence time at 380°C was less than 1 min. The heating and cooling profiles of the reactor were experimentally measured and are provided in Figure S1. The resulting biodiesel was dissolved in 3 mL of DCM and subjected to quantitative and qualitative analyses using GC/FID and GC/MS, respectively. The biodiesel yield was calculated, as described in Section 2.4.1. All experiments were performed in triplicate ($n = 3$), and the results are presented as mean ± standard deviation (SD). The numerical datasets, including mean values, SDs, and FAME compositions, are provided in Tables S8 and S9.

2.5 | Calculation of Fuel Properties of FAMEs and FAEEs

The fuel properties of FAMEs and FAEEs from noncatalytic transesterification of cottonseed oil were estimated using the reported prediction models. Parameters included lower heating value (LHV), cetane number, cold filter plugging point, density, flash point, iodine value, viscosity, and oxidative stability. The equations used to calculate the fuel properties of FAME and FAEE are summarized in Tables 1 and 2, respectively. In addition, input parameters used for fuel property prediction are presented in Tables S10 and S11.

3 | Results and Discussion

3.1 | TGA of Cottonseed and Cottonseed Oil

Cottonseed, a byproduct of cotton processing [22], is the fourth most produced oilseed after soybean, sunflower seed, and rapeseed, with a global production of approximately 40 million metric tons per year [37]. In contrast to other oils from seeds, cottonseed oil contains gossypol (a toxic polyphenolic compound), which limits its use as a cooking oil [38]. In this context, the direct conversion of crude, unrefined cottonseed oil into biodiesel could provide an alternative utilization pathway for cottonseed, a byproduct of the cotton fiber industry, and contribute to the diversification of biodiesel feedstocks [39]. To assess its potential as an oil source, TGA of cottonseed was conducted over the temperature range of 40–900°C (Figure 1a).

ijer, 2026, 1, Downloaded from https://onlinelibrary.wiley.com/doi/10.1155/er/8176983 by Hanyang University Library, Wiley Online Library on [16/11/2026]. See the Terms and Conditions (https://onlinelibrary.wiley.com/terms-and-conditions) on Wiley Online Library for rules of use; OA articles are governed by the applicable Creative Commons License

TABLE 1 | Equations used to estimate the fuel properties of fatty acid methyl esters (FAMEs).

Property	Equation	Ref.
Degree of unsaturation (UD)	$\sum$(unsaturated FA[a] × DB[b])	—
Length of chain (LC)	$\sum$(FA × Cn[c])	—
LHV (MJ kg^{-1})	$\sum$(FA × [0.03671 × molecular weight of FA × 0.9998^{DB} + 29.25 − 213.65 × wt. % of hydrogen atoms of FA − 0.77 × wt.% of oxygen atoms of FA])	[28, 29]
Cetane number	$\sum$(FA × [−21.157 + (7.965 − 1.785 × DB + 0.235 × DB^2) × Cn − 0.099 × Cn^2])	[30]
Cold filter plugging point (°C)	−0.488 × unsaturated FA + 36.0548	[31]
Density (kg m^{-3})	$\sum$(FA × [851.471 + (250.718 × DB + 280.899)/(1.214 + Cn)])	[32]
Flash point (°C)	1008.48 − LC × 136.166 + UD × 142.578 + LC^2 × 5.14811 − LC × UD × 10.6906 + UD^2 × 9.26352	[33]
Iodine value	254 × $\sum$(FA × DB/molecular weight of FAMEs)	[34]
Viscosity (mm^2 s^{-1})	$\sum$(FA × [0.04531 × molecular weight of FAMEs/1.07^{DB} − 7.853])	[28]
Oxidative stability (h)	$\sum$(FA × [60,060/(molecular weight of FAMEs$^{1.115}$ × 5.201^{DB}) + 3.852])	[28]

[a]FA is the content of fatty acid methyl esters, wt.%.
[b]DB is the number of double bonds of fatty acids.
[c]Cn is the number of carbon atoms of fatty acids.

TABLE 2 | Equations used to estimate the fuel properties of fatty acid ethyl esters (FAEEs).

Property	Equation	Ref.
Degree of unsaturation (UD)	$\sum$(unsaturated FA[a] × DB[b])	—
Length of chain (LC)	$\sum$(FA × Cn[c])	—
LHV (MJ kg^{-1})	$\sum$(FA × [0.04818 × molecular weight of FA × 0.9745^{DB} + 26.93 − 213.65 × wt. % of hydrogen atoms of FA − 0.77 × wt.% of oxygen atoms of FA])	[28, 29]
Cetane number	$\sum$(FA × [−15.027 + (7.641 − 1.522 × DB + 0.128 × DB^2) × Cn − 0.099 × Cn^2])	[30]
Cold filter plugging point (°C)	−103.47 − 0.59 × unsaturated FA + 7.3 × LC	[35]
Density (kg m^{-3})	$\sum$(FA × [851.471 + (250.718 × DB + 188.719)/(1.214 + Cn)])	[32]
Flash point (°C)	$\sum$(FA × [251.2 + 13.97 × Cn − 0.1198 × Cn^2 − 19.9 × DB])	[36]
Iodine value	254 × $\sum$ (FA × DB/molecular weight of FAEEs)	[34]
Viscosity (mm^2 s^{-1})	$\sum$ (FA × [0.0445 × molecular weight of FAEEs/1.06^{DB} − 8.085])	[28]
Oxidative stability (h)	$\sum$ (FA × [10,550/(molecular weight of FAMEs$^{1.115}$ × 4.405^{DB}) + 4.405])	[28]

[a]FA is the content of fatty acid ethyl esters, wt.%.
[b]DB is the number of double bonds of fatty acids.
[c]Cn is the number of carbon atoms of fatty acids.

At ≤530°C, 75.1 wt.% of the cottonseed mass was lost. In this range, the derivative thermogravimetric (DTG) peaks of cottonseed were observed at 224, 251, 328, and 395°C. Each DTG peak indicates the decomposition of specific constituents, which is used to identify the composition of the material [40]. Previous studies have reported that proteins and (hemi)cellulose decompose in the range of 200–400°C [41, 42]. Proteins are composed of peptide bonds with thermally unstable side chains, such as amide and carboxyl groups, while (hemi)cellulose consists of sugar units connected by strong glycosidic bonds [43, 44]. As such, proteins exhibit lower thermal stability than (hemi)cellulose, suggesting that the DTG peak at 224°C corresponds to the thermolysis of proteins. Hemicellulose is a branched heteropolysaccharide composed of various sugar monomers, such as xylose, mannose, and arabinose [45]. It has an amorphous structure and a lower degree of polymerization compared to cellulose, which contributes to its lower thermal stability [46]. Therefore, the DTG peaks observed at 251 and 328°C were likely attributed to the thermal decomposition of hemicellulose and cellulose, respectively. Lipids exhibit greater thermal stability than both proteins and (hemi)cellulose, typically undergoing thermolysis between 300–500°C [47]. As such, the highest DTG peak at 395°C was mainly attributed to the thermolysis of lipids. These TGA results suggest that the cottonseeds used in this study possess high potential as an oil-rich feedstock for biodiesel production. To verify this, oil was extracted from the cottonseeds using the Soxhlet extraction method and gravimetrically measured to be 23.8 ± 1.4 wt.%.

ijer, 2026, 1, Downloaded from https://onlinelibrary.wiley.com/doi/10.1155/er/8176983 by Hanyang University Library, Wiley Online Library on [16/11/2026]. See the Terms and Conditions (https://onlinelibrary.wiley.com/terms-and-conditions) on Wiley Online Library for rules of use; OA articles are governed by the applicable Creative Commons License

Considering that thermal energy drives the proposed noncatalytic transesterification, TGA was performed to characterize the thermolytic behavior of crude cottonseed oil, which may differ from that of refined oils, and to establish the reaction temperature range. Refined soybean oil was analyzed as a reference for comparison (Figure 1b). The mass loss of refined soybean oil occurred from 305 to 500°C, with a DTG peak observed at 419°C. Commercial refined vegetable oils such as soybean oil, canola oil, and sunflower oil are composed of triglycerides [48]. As such, the observed mass loss in soybean oil was attributed to the thermal decomposition of triglycerides [49]. Indeed, fatty acids are cleaved from the glycerol backbone during thermolysis [50]. The liberated fatty acids then volatilize, which causes mass loss [51]. The thermal decomposition pattern of cottonseed oil was similar to that of soybean oil in the temperature range of 305–500°C. However, additional mass loss was observed below 305°C, which can be attributed to the presence of FFAs in cottonseed oil. Note that the boiling points of FFAs range between 162–383°C [52]. The AV of cottonseed oil was determined to be 2.38 mg KOH g^{-1} oil, suggesting that FFA content of the oil was 1.19 wt.%. TGA analysis indicates that cottonseed oil was mainly composed of triglycerides with a small amount of FFAs.

3.2 | Noncatalytic Transesterification of Cottonseed Oil

In conventional base-catalyzed transesterification, cleavage of the ester bonds in triglycerides is a key step governing the overall conversion kinetics and is facilitated by the catalyst. As discussed in Section 3.1, thermal decomposition of triglycerides begins with cleavage of the ester bonds linking fatty acyl groups to the glycerol backbone at temperatures ≥305°C. Accordingly, it was hypothesized that thermal energy could facilitate this bond-cleavage step without a catalyst, thereby enabling thermally induced noncatalytic transesterification at temperatures above 305°C. The resulting fatty acid intermediates can subsequently react with alcohol to form fatty acid alkyl esters. Therefore, this study proposes a thermally induced noncatalytic transesterification pathway for FAEE production, in which thermal energy serves as the driving force for promoting transesterification. The proposed noncatalytic reaction, however, was conducted without external pressurization, which may lead to mass-transfer limitations between alcohol and fatty acid intermediates. At elevated reaction temperatures, the substantial difference in volatility between alcohol and fatty acid intermediates results in the more volatile alcohol exhibiting greater molecular mobility, whereas the less volatile oil phase remains comparatively less mobile [50]. Such differences in molecular mobility reduce the frequency of effective molecular collisions between the reactants, thereby limiting thermally induced noncatalytic transesterification [53]. Therefore, to enhance contact between the reactants, a porous material (silica) was introduced. The confined pore structure acts as a microreactor, increasing the frequency of effective molecular collisions between alcohol molecules and fatty acid intermediates, thereby promoting thermally induced noncatalytic transesterification [54]. The proposed reaction mechanism for

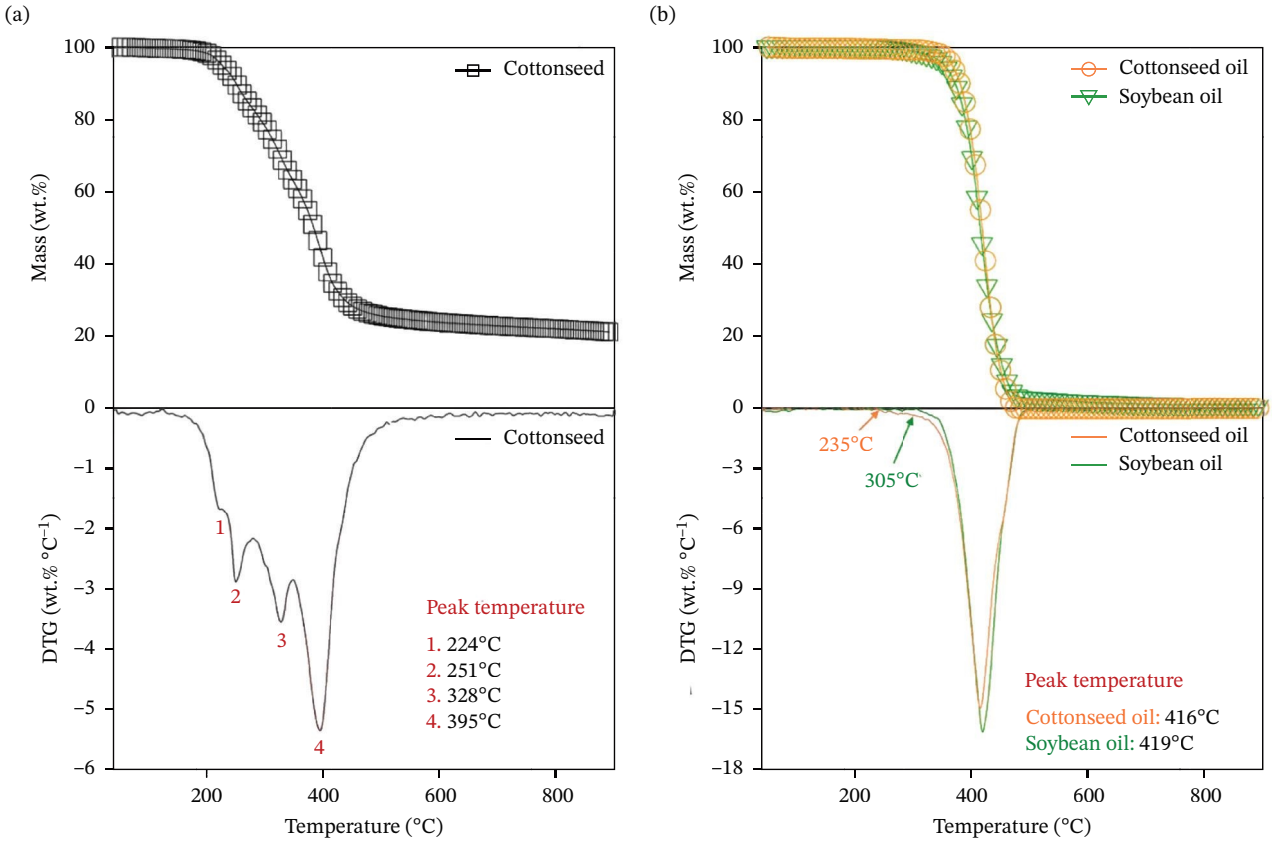

FIGURE 1 | Mass loss and derivative thermogravimetric (DTG) profiles of (a) cottonseed and (b) cottonseed oil and refined soybean oil as a function of temperature.

ijer, 2026, 1, Downloaded from https://onlinelibrary.wiley.com/doi/10.1155/er/8176983 by Hanyang University Library, Wiley Online Library on [16/11/2026]. See the Terms and Conditions (https://onlinelibrary.wiley.com/terms-and-conditions) on Wiley Online Library for rules of use; OA articles are governed by the applicable Creative Commons License

the thermally induced noncatalytic transesterification is illustrated in Figure S2.

To confirm the hypothesis, thermally induced noncatalytic transesterification of cottonseed oil was conducted using methanol or ethanol at 370°C for 1 min. This reaction temperature was selected to avoid thermal degradation of fatty acids as significant decomposition was observed above 400°C (Figure 1b). For comparison, conventional base-catalyzed transesterification of cottonseed oil was performed using methanol or ethanol over a reaction time of 120 min. In this study, cottonseed oil extracted from cottonseed by Soxhlet apparatus was used as feedstock for biodiesel production without further refining. The yields of FAMEs and FAEEs obtained from base-catalyzed and noncatalytic methods are shown in Figure 2a.

In the conventional catalytic method, methanol at an alcohol-to-oil molar ratio of 6:1 resulted in a FAME yield of 91.5 wt.% at 60°C for 120 min. In contrast, when ethanol was used at the same alcohol-to-oil molar ratio of 6:1, the FAEE yield was below 5 wt.% at 70°C for 120 min (data not shown). The lower FAEE yield was attributed to the slower reaction kinetics of ethanol in base-catalyzed transesterification [55]. To compensate for this limitation, an excess amount of ethanol was introduced, corresponding to an alcohol-to-oil molar ratio of 12:1. Under these conditions, the FAEE yield increased to 14.2 wt.%; however, the overall reactivity still remained lower than that observed with methanol. This reduced reactivity can be explained by the larger molecular size and longer alkyl chain of ethanol, which imposes greater steric hindrance and thereby hinders its effective interaction with the carbonyl groups of triglycerides relative to methanol [55, 56]. Noncatalytic transesterification achieved higher yields of FAMEs and FAEEs from cottonseed oil for a shorter reaction time compared to the conventional catalytic method. In particular, a FAME yield of 97.3 wt.% was achieved in 1 min at 370°C. Moreover, under the same conditions, the FAEE yield reached 77.8 wt.%, representing a more than 5.5-fold increase compared to the conventional method. These results suggest that the proposed noncatalytic method can overcome the limitations of base-catalyzed transesterification.

To clarify the role of the porous structure in thermally induced noncatalytic transesterification, a control experiment was conducted at 370°C using inert, nonporous glass beads. Both FAME and FAEE yields remained below 25 wt.%, substantially lower than those obtained with porous silica. The low biodiesel yields indicate that, although thermal energy initiates transesterification, efficient biodiesel formation is favored by the presence of a porous structure. Nevertheless, because surface acid sites or silanol groups on silica may potentially contribute to transesterification, additional control experiments were conducted for FAEE production at 370°C using nonporous silica and in the absence of silica. The FAEE yields obtained with nonporous silica and without silica were 15.5 and 18.3 wt.%, respectively. Although a contribution from surface acid or silanol sites cannot be completely excluded, the FAEE yield was slightly higher in the absence of any solid material than in the presence of nonporous silica, suggesting that these sites are unlikely to be a major factor

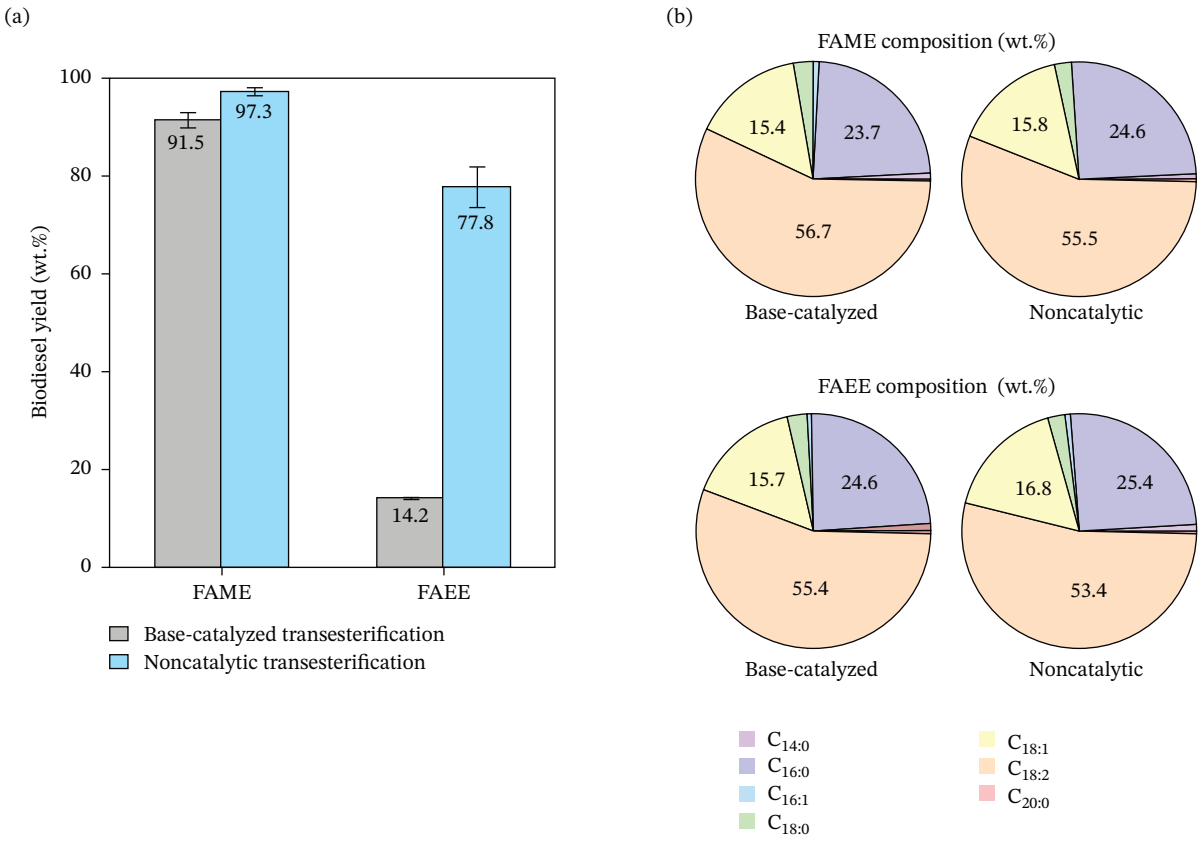

FIGURE 2 | (a) Yields of FAME and FAEE produced from cottonseed oil via base-catalyzed and noncatalytic transesterification and (b) corresponding fatty acid compositions of the obtained biodiesel products. Experimental results are presented as mean ± SD ($n = 3$) with SD values below 3%.

ijer, 2026, 1, Downloaded from https://onlinelibrary.wiley.com/doi/10.1155/er/8176983 by Hanyang University Library, Wiley Online Library on [16/11/2026]. See the Terms and Conditions (https://onlinelibrary.wiley.com/terms-and-conditions) on Wiley Online Library for rules of use; OA articles are governed by the applicable Creative Commons License

in enhancing FAEE formation. These results support an important role of the porous structure of silica and its associated confinement effect in enhancing biodiesel formation by promoting effective contact between reactants and increasing the frequency of molecular collisions. The effect of the ethanol-to-oil molar ratio on FAEE yield over the range of 50:1–568:1 is provided in Figure S3. FAEE yield increased with the ethanol-to-oil molar ratio up to 300:1 and remained nearly constant at higher ratios. To provide a deeper understanding of the reaction mechanism, comprehensive kinetic studies, including reaction-time optimization, determination of reaction rate constants, activation energy, and kinetic modeling, should be conducted in future work. Moreover, further mechanistic verification using in situ spectroscopic techniques (e.g., in situ FT-IR) or other operando analyses capable of monitoring reaction intermediates is required in future studies to validate the proposed reaction pathway.

The main components of biodiesel derived from cottonseed oil were palmitic acid ($C_{16:0}$), oleic acid ($C_{18:1}$), and linoleic acid ($C_{18:2}$) (Figure 2b). Since the double bonds in oleic acid and linoleic acid are thermally unstable, the relatively high reaction temperature of the noncatalytic process could potentially alter the fatty acid composition of the resulting FAMEs/FAEEs. Contrary to this concern, the fatty acid compositions were nearly identical for base-catalyzed and noncatalytic transesterification. This indicates that noncatalytic method can effectively convert cottonseed oil into biodiesel without thermally altering its composition.

Nevertheless, the FAEE yield from the noncatalytic process was still low (< 80 wt.%). Because this reaction is driven by heat, higher temperatures may increase the collision frequency between ethanol and cottonseed oil, which raises the FAEE yield. To determine the optimal reaction temperature, noncatalytic transesterification of cottonseed oil was conducted using ethanol at temperatures ranging from 250 to 390°C (Figure 3a).

As shown in Figure 3a, negligible FAEE formation was observed below 300°C despite continuous thermal exposure during the heating period (Figure S1). Once the reaction temperature exceeded 300°C, the FAEE yield increased rapidly, reaching a maximum of 88.1 wt.% at 380°C. These results demonstrate that the proposed thermally induced noncatalytic transesterification is governed by reaction temperature rather than cumulative thermal exposure time. At elevated temperatures, sufficient thermal energy promotes ester bond cleavage in triglycerides and increases the frequency of effective molecular collisions, thereby enabling rapid transesterification within a short residence time. Even at higher reaction temperatures (390°C), the FAEE yield remained below 90 wt.%. This lower yield may be attributed to (i) thermal cracking of FAEEs at elevated temperatures or (ii) the inherently lower reactivity of ethanol compared to methanol with fatty acids in transesterification. To investigate the possibility of thermal cracking, the composition of FAEEs was examined (Figure 3b). While linoleic acid ($C_{18:2}$) is thermally unstable [57], no evidence of thermal cracking of linoleic acid ethyl esters was observed at elevated reaction temperatures ≥ 380°C. In addition, the FAEE composition at 380°C was 52.9 wt.% linoleic acid, 25.7 wt.% palmitic acid, and 17.0 wt.% oleic acid, which was similar to the FAME composition. Consistent with these observations, GC/MS analysis of the reaction products (Figure S4) detected only trace amounts of volatile cracking products, indicating that the thermal degradation of FAEEs was not significant under the investigated reaction conditions. These results suggest that the lower FAEE yield compared to FAME yield is more likely due to the lower reactivity of ethanol in transesterification rather than thermal degradation of FAEEs.

To explore the relative reactivity of ethanol compared to methanol, noncatalytic transesterification of cottonseed oil was carried out at 380°C using three methanol-to-ethanol molar ratios. As shown in Figure 4, the peak areas corresponding to FAMEs were larger than those of FAEEs at identical molar ratios of methanol

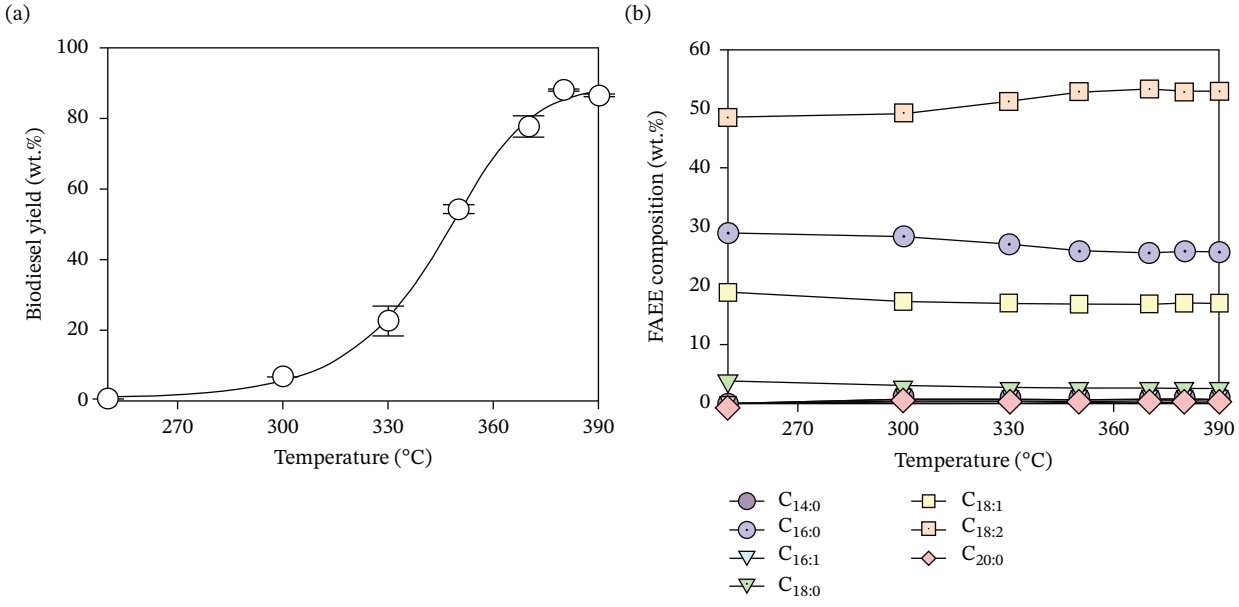

FIGURE 3 | (a) Yield and (b) composition of FAEEs produced via noncatalytic transesterification of cottonseed oil as a function of temperature. Experimental results are presented as mean ± SD ($n = 3$) with SD values below 5%.

ijer, 2026, 1, Downloaded from https://onlinelibrary.wiley.com/doi/10.1155/er/8176983 by Hanyang University Library, Wiley Online Library on [16/11/2026]. See the Terms and Conditions (https://onlinelibrary.wiley.com/terms-and-conditions) on Wiley Online Library for rules of use; OA articles are governed by the applicable Creative Commons License

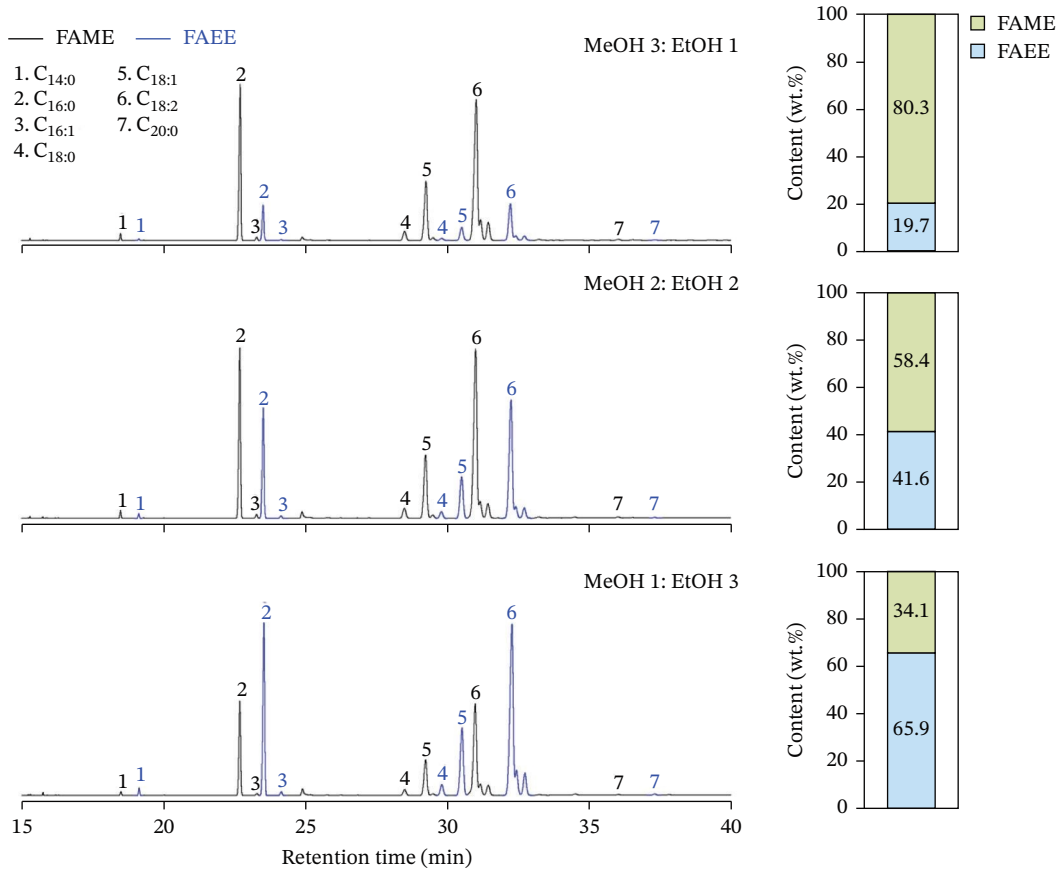

FIGURE 4 | Chromatogram of FAME and FAEE mixtures obtained from cottonseed oil by noncatalytic transesterification under varying methanol (MeOH)-to-ethanol (EtOH) molar ratios with a comparison of the FAME and FAEE contents. Experimental results are presented as mean ± SD ($n = 3$) with SD values below 3%.

and ethanol. This difference was evident in the peaks associated with palmitic acid and linoleic acid esters. As the proportion of ethanol increased, the FAEE content also increased. However, when methanol and ethanol were used in an equimolar ratio (2:2), the resulting biodiesel contained 58.4 wt.% FAMEs and 41.6 wt.% FAEEs, indicating the relatively lower reactivity of ethanol in transesterification. Therefore, although increasing the reaction temperature improved the FAEE yield, further studies are needed to systematically investigate operating parameters beyond reaction temperature to better understand the reaction characteristics of ethanol-based thermally induced noncatalytic transesterification. Despite the lower reactivity of ethanol, the FAEE yield obtained through noncatalytic transesterification (88.1 wt.%) was higher and achieved in a shorter reaction time than those reported in previous studies using ethanol with other inedible oils (53.2–86.0 wt.% over 20–120 min) [58–60]. This suggests that ethanol-based noncatalytic transesterification provides a more efficient pathway for converting inedible oil such as cottonseed oil into biodiesel.

3.3 | Effect of Impurity Content on FAEE Yield

Ethanol produced via biomass fermentation is purified by distillation [61]; however, conventional distillation yields an azeotropic mixture containing 96 wt.% ethanol and 4 wt.% water. In other words, achieving ethanol purity beyond 96 wt.% through distillation is limited [62]. In base-catalyzed transesterification, water induces the hydrolysis of triglycerides and FAEEs, forming FFAs, which subsequently react with catalysts through saponification [63]. This side reaction decreases the biodiesel yield. Zhang et al. [64] reported that oils used in base-catalyzed transesterification should have a water content below 1 wt.%. Therefore, a conversion method capable of achieving a high FAEE conversion efficiency with water-containing ethanol is needed. To evaluate the water tolerance of the noncatalytic process, transesterification was conducted by adding 2–10 wt.% water to ethanol and reacting it with cottonseed oil (Figure 5a).

As shown in Figure 5a, the FAEE yield was decreased from 88.1 to 76.9 wt.% as the water content increased from 0 to 10 wt.%. Nevertheless, 96 wt.% ethanol, corresponding to the practical purity limit attainable by conventional distillation, achieved an FAEE yield of 85.4 wt.%, comparable to the 88.1 wt.% obtained using anhydrous ethanol. Furthermore, the composition of FAEEs was nearly identical to the results shown from the noncatalytic transesterification of cottonseed oil (Figure 3b). These results demonstrate that FAEEs can be produced using ethanol with a purity achievable by conventional distillation, while maintaining a yield close to that obtained with anhydrous ethanol. Thus, additional ethanol dehydration may not be necessary. The consistent FAEE yield also suggests that FFAs generated by hydrolysis were effectively converted into biodiesel. To verify this, noncatalytic transesterification of cottonseed oil with the addition of 2–10 wt.% linoleic acid as FFAs was conducted. As

ijer, 2026, 1, Downloaded from https://onlinelibrary.wiley.com/doi/10.1155/er/8176983 by Hanyang University Library, Wiley Online Library on [16/11/2026]. See the Terms and Conditions (https://onlinelibrary.wiley.com/terms-and-conditions) on Wiley Online Library for rules of use; OA articles are governed by the applicable Creative Commons License

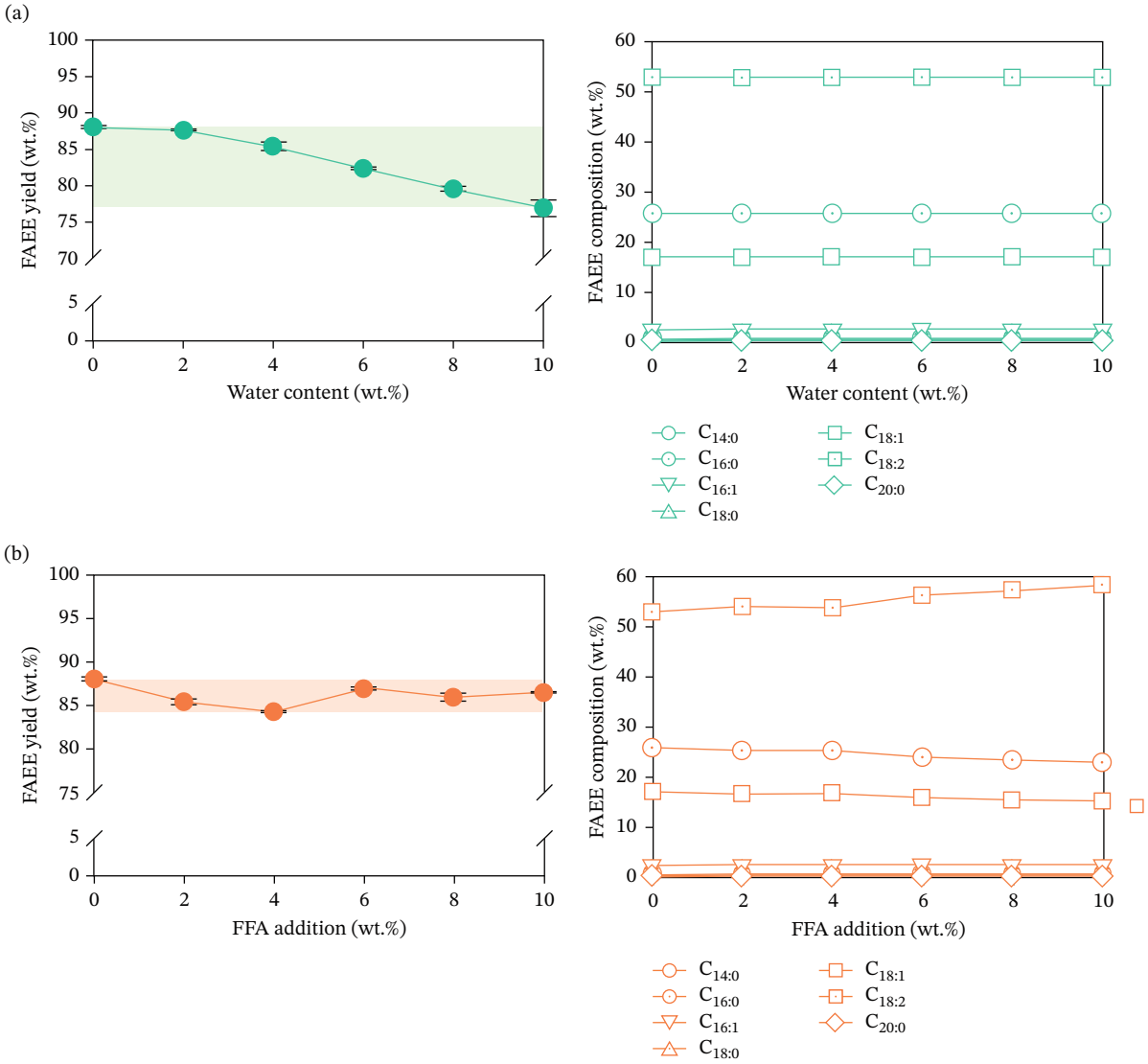

FIGURE 5 | Yield and composition of FAEEs produced via noncatalytic transesterification of cottonseed oil as a function of (a) water and (b) FFA addition. Experimental results are presented as mean ± SD ($n = 3$) with SD values below 2%.

shown in Figure 5b, the FAEE yield ranged from 84.3 to 88.1 wt.% across the investigated FFA contents, with composition changes relative to Figure 3b being negligible. These results indicate that FFAs were converted into FAEEs through esterification. To evaluate the statistical significance of the effects of water content and FFA addition on FAEE production, one-way analysis of variance (ANOVA) was performed (Tables S12 and S13). The ANOVA results revealed statistically significant differences for both water content and FFA addition ($p < 0.001$). Although water content had a statistically significant effect on FAEE yield, high biodiesel yields were maintained up to 96 wt.% ethanol. Since 96 wt.% ethanol corresponds to the ethanol–water azeotropic composition and represents the highest purity obtainable by conventional distillation, this result demonstrates the robustness of the proposed process toward industrial-grade water-containing ethanol. ANOVA also indicated a statistically significant effect of FFA addition. However, the actual difference in FAEE yield was small, with values ranging from 84.3 to 88.1 wt.%. This indicates that the statistical significance was largely attributable to the small within-group variation rather than a substantial change in the process performance. Therefore, the proposed process maintained consistently high FAEE yields across the investigated FFA range.

Generally, oils with high FFA contents require an acid-catalyzed esterification pretreatment to remove FFAs prior to base-catalyzed transesterification [65]. However, acid-catalyzed esterification requires long reaction times (2–5 h) [66], and the acidic wastewater generated during the washing process to remove salts from the resulting products imposes additional economic and environmental burdens in the biodiesel industry [67]. In contrast, the noncatalytic transesterification enables simultaneous esterification of FFAs and transesterification of triglycerides in a single step within a short reaction time. Therefore, catalyst removal through washing is unnecessary, thereby reducing wastewater generation and the associated economic and environmental burdens. In addition, considering that soap formation resulting from the reaction between FFAs and base catalysts hinders phase separation between biodiesel and glycerol, biodiesel production via thermally induced noncatalytic transesterification may reduce the cost of downstream processing for the recovery of high-purity glycerol. However, future studies should include purity analysis

ijer, 2026, 1, Downloaded from https://onlinelibrary.wiley.com/doi/10.1155/er/8176983 by Hanyang University Library, Wiley Online Library on [16/11/2026]. See the Terms and Conditions (https://onlinelibrary.wiley.com/terms-and-conditions) on Wiley Online Library for rules of use; OA articles are governed by the applicable Creative Commons License

of the recovered biodiesel to determine the remaining water after transesterification using water-containing ethanol.

3.4 | Comparison of Fuel Properties Between FAMEs and FAEEs

To enable the practical application of FAEEs, its physicochemical properties should meet fuel quality standards such as ASTM D6751 and EN 14214 [68]. In this context, the key physicochemical properties of FAEEs produced via noncatalytic transesterification of cottonseed oil using ethanol were estimated using the equations provided in Tables 1 and 2. These predicted properties were then compared with those of FAMEs derived from the noncatalytic transesterification of cottonseed oil. The estimated values are summarized in Table 3.

Table 3 shows that the fuel properties of the produced FAEE are predicted to fall within the specification ranges of ASTM D6751 and EN 14214. In addition, FAEEs exhibited improved fuel performance compared to that of FAMEs. Previous studies have also reported that FAEEs possesses higher LHV, cetane number, flash point, viscosity, and oxidative stability, while showing lower cold filter plugging point, density, and iodine value than FAMEs [69–71]. These enhanced properties are attributed to the additional $-CH_2$ group in FAEEs, as LHV, cetane number, flash point, and oxidative stability generally increase with carbon chain length [72–74]. Moreover, the ethyl group, having a longer chain than the methyl group, enhances hydrophobic interactions and disrupts the interaction between oxygen atoms and alkyl chains that promote solid formation [73]. This effect lowers the solidification temperature, thereby improving cold-flow performance and resulting in a lower cold filter plugging point than FAMEs [73]. The higher molecular weight of FAEEs compared to FAMEs strengthens the van der Waals forces between molecules, increasing viscosity; however, the reduced molecular packing efficiency leads to a lower density [75]. However, it should be noted that these fuel properties were estimated using established predictive models primarily based on the fatty acid ester composition of the produced biodiesel. These models do not fully account for the effects of minor constituents in biodiesel, which may cause discrepancies between predicted and experimentally measured values. In addition, biodiesel standards, such as ASTM D6751 and EN 14214, include parameters beyond the predicted properties presented in this study, including ester content, AV, water content, free and total glycerol, and residual alcohol. Therefore, these properties should be experimentally determined in future studies to provide a rigorous evaluation of the fuel quality and practical applicability of the produced biodiesel.

To benchmark the proposed process against existing FAEE production technologies, the FAEE yields and reaction conditions were compared with those reported for catalytic and noncatalytic transesterification processes (Table 4). Conventional base-catalyzed transesterification generally produces FAEE yields of 53.2–90.3 wt.% at 65–70°C but typically requires reaction times of up to 180 min. Previously reported noncatalytic transesterification processes eliminate the need for catalysts and shorten the reaction time to 30–45 min; however, they are conducted under supercritical conditions with externally applied pressures of 34–300 bar to achieve FAEE yields of 68.9–85.3 wt.%. In contrast, the proposed thermally induced noncatalytic transesterification achieved an FAEE yield of 88.1 wt.% within 1 min without externally applied pressure. These comparisons indicate that the proposed process achieves an FAEE yield comparable to or higher than those reported for conventional catalytic and noncatalytic processes while avoiding both catalyst use and external pressurization. Although an autogenous pressure of 247 bar was estimated to develop within the sealed reactor at 380°C, temperature is considered the primary reaction parameter in the proposed process. Our previous studies on thermally induced transesterification demonstrated that biodiesel production (>95 wt.%) could be achieved at atmospheric pressure (1 bar) [79, 80]. Although the proposed process demonstrates the potential of thermally induced noncatalytic transesterification, comprehensive techno-economic analyses are required to determine whether the proposed process offers practical advantages over conventional catalytic and supercritical transesterification. Such an analysis should consider heat input and recovery, alcohol recovery and recycling, product purification, reactor design, and process integration in future work.

3.5 | Contribution of CO_2 Emission Reduction

In commercially established biodiesel production processes, methanol is predominantly used as the alcohol feedstock. However, conventional methanol is generally synthesized from natural gas, and its manufacture accounts for 0.706 kg of CO_2 emissions generated during the production of 1 kg of biodiesel

TABLE 3 | Physicochemical properties of FAME and FAEE derived from cottonseed oil.

Property	FAME	FAEE	ASTM D6751	EN 14214
LHV (MJ kg−1)	39.8	41.0	—	>35
Cetane number	56.9	58.7	>47	>51
Cold filter plugging point (°C)	1.0	−3.8	<5	—
Density ($kg\,m^{-3}$)	883.2	878.3	880	860–900
Flash point (°C)	157.8	160.1	>130	>101
Iodine value ($g\,I_2\,100\,g^{-1}$)	109.7	104.8	—	<120
Viscosity ($mm^2\,s^{-1}$)	4.1	4.5	1.9–6.0	3.5–5.0
Oxidative stability (h)	9.5	10.9	>3	>8

ijer, 2026, 1, Downloaded from https://onlinelibrary.wiley.com/doi/10.1155/er/8176983 by Hanyang University Library, Wiley Online Library on [16/11/2026]. See the Terms and Conditions (https://onlinelibrary.wiley.com/terms-and-conditions) on Wiley Online Library for rules of use; OA articles are governed by the applicable Creative Commons License

TABLE 4 | Comparison of the thermally induced noncatalytic transesterification with previously reported catalytic and noncatalytic processes for FAEE production.

Feedstock	Catalyst	Reaction conditions	FAEE yield (wt.%)	Ref.
Catalytic transesterification				
Grape seed oil	$NaOC_2H_5$	70°C, 180 min	90.3	[76]
Canola oil	NaOH	70°C, 20 min	85.4	[58]
Tung oil	NaOH	70°C, 20 min	53.2	[58]
Karanja oil	KOH	65°C, 90 min	78.1	[59]
Noncatalytic transesterification				
Camelina sativa oil	—	290°C, 30 min, 34 bar (externally applied)	85.3	[77]
Rapeseed oil	—	380°C, 30 min, 300 bar (externally applied)	77.5	[18]
Crambe oil	—	300°C, 45 min, 200 bar (externally applied)	79.3	[78]
Cottonseed oil	—	380°C, ≤1 min, 247 bar (estimated autogenous)	88.1	This study

[81]. Consequently, the overall carbon mitigation benefits of biodiesel are diminished. In contrast, ethanol obtained via fermentation of biomass can enhance the environmental performance of biodiesel, reducing CO_2 emissions by 2.454 kg per kg of biodiesel [81]. Figure 6a compares the potential of CO_2 emission mitigation associated with replacing conventional diesel fuel with FAME and FAEE produced through the noncatalytic transesterification of cottonseed oil. Detailed input parameters used for calculation of CO_2 emissions are presented in Table S14.

The LHV of FAME and FAEE converted from cottonseed oil were 39.8 and 41.0 MJ kg^{-1}, respectively (Table 3). Based on the annual cottonseed production of 41.29 Mt, the estimated production amounts of FAME and FAEE through noncatalytic transesterification were estimated at 9.56 and 8.66 Mt, respectively [37]. Accordingly, the total recoverable energy was calculated to be 380.56 PJ for FAME and 354.96 PJ for FAEE. These energy outputs are equivalent to those obtained from the consumption of 8.87 and 8.27 Mt of diesel fuel, respectively. Therefore, substituting fossil-derived diesel fuel with biodiesel could reduce CO_2 emissions by 0.69 g $g_{Seed}^{-1}$for FAME and 0.64 g $g_{Seed}^{-1}$for FAEE (Equation S1). Considering that the CO_2 emissions associated with alcohol production are 0.17 g g_{Seed}^{-1} for methanol and −0.52 g $g_{Seed}^{-1}$for ethanol (Equation S2), the net CO_2 emissions achieved through FAEE production is higher than that obtained through FAME production. Consequently, the FAEE production pathway can contribute to lower CO_2 emissions than the FAME production pathway. However, the system boundary for estimating the potential CO_2 mitigation was limited to petroleum diesel displacement on an equivalent-energy basis and the CO_2 emissions associated with alcohol production. In addition, CO_2 emissions from biodiesel combustion were excluded based on the assumption that the biogenic carbon released during combustion is offset by CO_2 uptake during biomass growth. Therefore, the calculated values represent a preliminary estimate within the defined system boundary rather than a comprehensive life-cycle assessment. For a more practical evaluation of the environmental performance, process-related emissions arising from heating, alcohol and solvent recovery, silica production and reuse, oil extraction, and product purification, as well as the allocation of environmental burdens to cottonseed, should be incorporated into a comprehensive life-cycle assessment in future work.

Figure 6b illustrates a schematic overview of FAEE production via the noncatalytic transesterification of cottonseed oil. The cotton fiber industry generates substantial quantities of cottonseed as a byproduct. From this resource, approximately 9.83 Mt of oil can be supplied annually as a biodiesel feedstock. Cottonseed oil is subsequently converted into the renewable fuel FAEE through the reaction with ethanol under noncatalytic transesterification conditions. Even though ethanol recovered by distillation after fermentation typically contains at least 4 wt.% water, the FAEE yield with ethanol containing 4 wt.% water was comparable to that obtained using anhydrous ethanol under noncatalytic conditions. The use of 96 wt.% ethanol has the potential to reduce the energy consumption associated with ethanol dehydration. Furthermore, the reaction was completed within less than 1 min after reaching the target temperature, thereby reducing heat input during the residence time. These characteristics of the proposed process may contribute to reducing the overall energy demand despite the relatively high temperatures required for operation. Thus, the proposed process represents a promising route for FAEE production. Moreover, its implementation could further enhance carbon emission reduction within the biodiesel industry. Nevertheless, comprehensive energy balance analysis, including heat input, heat recovery, and process integration, will be required to quantitatively assess the overall energy demand and industrial applicability of the proposed process. Furthermore, the present study was conducted at the laboratory scale using a 1 mL reactor, and further scale-up studies are therefore required. As reactor size increases, temperature gradients may develop, leading to heat-transfer limitations that can influence the thermal cleavage of ester bonds and the overall reaction efficiency. Accordingly, practical implementation of the

ijer, 2026, 1, Downloaded from https://onlinelibrary.wiley.com/doi/10.1155/er/8176983 by Hanyang University Library, Wiley Online Library on [16/11/2026]. See the Terms and Conditions (https://onlinelibrary.wiley.com/terms-and-conditions) on Wiley Online Library for rules of use; OA articles are governed by the applicable Creative Commons License

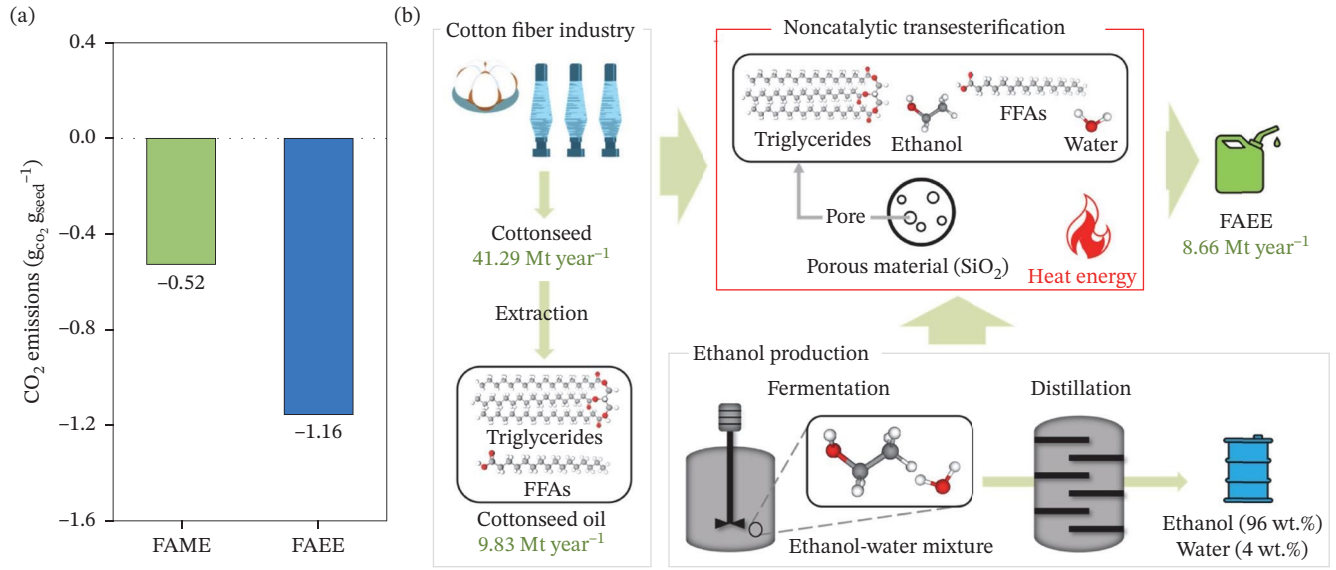

FIGURE 6 | (a) Potential for CO_2 emission mitigation through the use of FAME or FAEE as alternative diesel fuels and (b) schematic diagram of the FAEE production process via noncatalytic transesterification of cottonseed oil.

proposed process will require systematic optimization of reactor design and operating conditions through reactor scale-up combined with thermal-fluid analysis.

4 | Conclusions

This study employed noncatalytic transesterification to produce ethanol-based biodiesel (FAEEs). Noncatalytic reaction achieved a FAEE yield of 88.1 wt.% at 380°C in 1 min, whereas FAEE synthesis was limited under conventional base-catalyzed conditions, resulting in a yield of only 14.2 wt.%. This suggests that the proposed noncatalytic method enhanced mass transfer between cottonseed oil and ethanol. In addition, significant thermal degradation of FAEEs was not evident despite the higher reaction temperatures. Given that fermentation-derived ethanol contains at least 4 wt.% water due to the ethanol–water azeotrope, this study evaluated the potential of producing biodiesel with ethanol that contains water. The noncatalytic process achieved an FAEE yield of 85.4 wt.% with ethanol containing 4 wt.% water, approaching that obtained with anhydrous ethanol. This result suggests that noncatalytic transesterification could be a promising strategy for producing FAEEs using water-containing ethanol. Moreover, the noncatalytic process using ethanol mitigated CO_2 emissions by 1.16 $g\,g_{Seed}^{-1}$. Thus, the noncatalytic process with ethanol offers both technical and environmental advantages. Nevertheless, further investigation is required to establish the practical applicability of the proposed process, including optimization of the reactant loading and reactor configuration, process scale-up, energy balance, alcohol recovery, silica reuse, and techno-economic and life-cycle assessments.

Acknowledgments

This work was supported by the National Research Foundation of Korea (NRF) grants funded by the Korean Government (MSIT) (Grants RS-2023-NR077231 and RS-2025-00556963) and the Basic Science Research Program through the National Research Foundation of Korea (NRF) funded by the Ministry of Education (Grant RS-2025-25428562).

Funding

This work was funded by the National Research Foundation of Korea (NRF) grants funded by the Korean Government (MSIT) (Grants RS-2023-NR077231 and RS-2025-00556963) and the Basic Science Research Program through the National Research Foundation of Korea (NRF) funded by the Ministry of Education (Grant RS-2025-25428562).

Conflicts of Interest

The authors declare no conflicts of interest.

Data Availability Statement

The data will be made available upon request.

References

1. United States Environmental Protection Agency, *Overview of Greenhouse Gases*, (2025).

2. M. Khan, X. Sun, A. Zada, et al., "Carbon Dioxide, Global Boiling, and Climate Carnage, From Generation to Assimilation, Photocatalytic Conversion to Renewable Fuels, and Mechanism," *Science of the Total Environment* 965 (2025): 178629.

3. International Energy Agency, "Electricity Mid-Year Update," (2024).

4. I. Nordin, K. Elofsson, and T. Jansson, "Cost-Effective Reductions in Greenhouse Gas Emissions: Reducing Fuel Consumption or Replacing Fossil Fuels With Biofuels," *Energy Policy* 190 (2024): 114138.

5. G. Kalghatgi, "Development of Fuel/Engine Systems—The Way Forward to Sustainable Transport," *Engineering* 5, no. 3 (2019): 510–518.

6. Y. Liu, Z. Zhu, J. Shi, S. Zhao, F. Liu, and H. Jin, "Facile Synthesis and Economic Analysis of Cu/C Catalyst for Efficient Biodiesel Production," *International Journal of Energy Research* 46, no. 14 (2022): 19814–19825.

7. I. Chanakaewsomboon, K. Phoungthong, A. Palamanit, V. Seechamnanturakit, and C. K. Cheng, "Biodiesel Produced Using Potassium Methoxide Homogeneous Alkaline Catalyst: Effects of Various Factors on Soap Formation," *Biomass Conversion and Biorefinery* 13, no. 10 (2023): 9237–9247.

ijer, 2026, 1, Downloaded from https://onlinelibrary.wiley.com/doi/10.1155/er/8176983 by Hanyang University Library, Wiley Online Library on [16/11/2026]. See the Terms and Conditions (https://onlinelibrary.wiley.com/terms-and-conditions) on Wiley Online Library for rules of use; OA articles are governed by the applicable Creative Commons License

8. Monika, S. Banga, and V. V. Pathak, "Biodiesel Production From Waste Cooking Oil: A Comprehensive Review on the Application of Heterogenous Catalysts," *Energy Nexus* 10 (2023): 100209.

9. T. Blumberg, G. Tsatsaronis, and T. Morosuk, "On the Economics of Methanol Production From Natural Gas," *Fuel* 256 (2019): 115824.

10. O. Yadav, H. Valera, D. Dulani, U. Krishnan, and A. Kumar Agarwal, "Safety Aspects of Methanol as Fuel," in *Methanol: A Sustainable Transport Fuel for CI Engines*, ed. A. K. Agarwal, (2021): 117–138.

11. Y. S. Erchamo, T. T. Mamo, G. A. Workneh, and Y. S. Mekonnen, "Improved Biodiesel Production From Waste Cooking Oil With Mixed Methanol–Ethanol Using Enhanced Eggshell-Derived CaO Nano-Catalyst," *Scientific Reports* 11, no. 1 (2021): 6708.

12. H. Kazemi Shariat Panahi, M. Dehhaghi, G. J. Guillemin, et al., "Bioethanol Production From Food Wastes Rich in Carbohydrates," *Current Opinion in Food Science* 43 (2022): 71–81.

13. P. A. Leggieri, M. Senra, and L. Soh, "Cloud Point and Crystallization in Fatty Acid Ethyl Ester Biodiesel Mixtures With and Without Additives," *Fuel* 222 (2018): 243–249.

14. V. Mandari and S. K. Devarai, "Biodiesel Production Using Homogeneous, Heterogeneous, and Enzyme Catalysts via Transesterification and Esterification Reactions: A Critical Review," *BioEnergy Research* 15, no. 2 (2022): 935–961.

15. H. Zentou, Z. Abidin, R. Yunus, D. Awang Biak, and D. Korelskiy, "Overview of Alternative Ethanol Removal Techniques for Enhancing Bioethanol Recovery From Fermentation Broth," *Processes* 7, no. 7 (2019): 458.

16. R. S. Abusweireh, N. Rajamohan, and Y. Vasseghian, "Enhanced Production of Biodiesel Using Nanomaterials: A Detailed Review on the Mechanism and Influencing Factors," *Fuel* 319 (2022): 123862.

17. H. C. Nguyen, J-W. Pan, C-H. Su, H. C. Ong, J-M. Chern, and J-Y. Lin, "Sol-Gel Synthesized Lithium Orthosilicate as a Reusable Solid Catalyst for Biodiesel Production," *International Journal of Energy Research* 45, no. 4 (2021): 6239–6249.

18. S. V. Mazanov, A. R. Gabitova, R. A. Usmanov, et al., "Continuous Production of Biodiesel From Rapeseed Oil by Ultrasonic Assist Transesterification in Supercritical Ethanol," *The Journal of Supercritical Fluids* 118 (2016): 107–118.

19. N. Akkarawatkhoosith, A. Kaewchada, and A. Jaree, "Production of Biodiesel From Palm Oil Under Supercritical Ethanol in the Presence of Ethyl Acetate," *Energy & Fuels* 33, no. 6 (2019): 5322–5331.

20. O. V. Okoro, F. A. Santos-Bastilla, A. Amenaghawon, L. Nie, and A. Shavandi, "Integrated Optimization and Simulation of Biodiesel Production With Conceptual Anaerobic Digestion: A Techno-Economic Assessment for Circular Bioenergy Recovery," *Chemical Engineering Research and Design* 224 (2025): 561–574.

21. M. G. Nayak, "Review and Comparison of the Methodology Adopted for Biodiesel Production," *Carbon Resources Conversion* 9, no. 1 (2026): 100343.

22. M. Negm and S. Sanad, "1—Cotton Fibres, Picking, Ginning, Spinning and Weaving," in *Handbook of Natural Fibres*, 2 ed., eds. R. M. Kozłowski and M. Mackiewicz-Talarczyk, (Woodhead Publishing, 2020): 3–48.

23. I. Sharif, J. Farooq, S. M. Chohan, et al., "Strategies to Enhance Cottonseed Oil Contents and Reshape Fatty Acid Profile Employing Different Breeding and Genetic Engineering Approaches," *Journal of Integrative Agriculture* 18, no. 10 (2019): 2205–2218.

24. K. Mohan, P. Sathishkumar, D. K. Rajan, J. Rajarajeswaran, and A. R. Ganesan, "Black Soldier Fly (*Hermetia illucens*) Larvae as Potential Feedstock for the Biodiesel Production: Recent Advances and Challenges," *Science of the Total Environment* 859 (2023): 160235.

25. X. Liu, G. Michal, A. Godbole, and C. Lu, "Decompression Modelling of Natural Gas-Hydrogen Mixtures Using the Peng-Robinson Equation of State," *International Journal of Hydrogen Energy* 46, no. 29 (2021): 15793–15806.

26. L. P. Ramos, L. F. Maia, M. Z. Andreatta Callegari, T. A. Da Silva, J. Bressiani, and A. Zandoná Filho, "Cellulosic Ethanol Production Using Five Commercial Varieties of Energycane," *Industrial Crops and Products* 224 (2025): 120403.

27. M. L. Motloutsi, F. Matebese, M. J. Madito, M. M. Motsa, M. Managa, and R. M. Moutloali, "Zwitterion Functionalized Graphene Oxide Thin Film Nanocomposite Membrane for Brackish Water Desalination and Natural Organic Matter Removal," *Desalination and Water Treatment* 323 (2025): 101276.

28. I. K. Hong, J. R. Lee, and S. B. Lee, "Fuel Properties of Canola Oil and Lard Biodiesel Blends: Higher Heating Value, Oxidative Stability, and Kinematic Viscosity," *Journal of Industrial and Engineering Chemistry* 22 (2015): 335–340.

29. A. Llamas, M. D. Lapuerta, A.-M. D. Al-Lal, and L. Canoira, "Oxygen Extended Sooting Index of FAME Blends With Aviation Kerosene," *Energy & Fuels* 27, no. 11 (2013): 6815–6822.

30. M. Lapuerta, J. Rodríguez-Fernández, and E. F. de Mora, "Correlation for the Estimation of the Cetane Number of Biodiesel Fuels and Implications on the Iodine Number," *Energy Policy* 37, no. 11 (2009): 4337–4344.

31. C. Caldeira, F. Freire, E. A. Olivetti, and R. Kirchain, "Fatty Acid Based Prediction Models for Biodiesel Properties Incorporating Compositional Uncertainty," *Fuel* 196 (2017): 13–20.

32. M. Lapuerta, J. Rodríguez-Fernández, and O. Armas, "Correlation for the Estimation of the Density of Fatty Acid Esters Fuels and Its Implications. A Proposed Biodiesel Cetane Index," *Chemistry and Physics of Lipids* 163, no. 7 (2010): 720–727.

33. S. Pinzi, D. Leiva, G. Arzamendi, L. M. Gandia, and M. P. Dorado, "Multiple Response Optimization of Vegetable Oils Fatty Acid Composition to Improve Biodiesel Physical Properties," *Bioresource Technology* 102, no. 15 (2011): 7280–7288.

34. J. L. Guil-Guerrero, M. D. J. Sánchez-Muros, D. Fabrikov, et al., "*Hermetia illucens* Larvae as a Living Bioreactor for Simultaneous Food By-Products Recycling and Useful Oil Production," *Journal of the American Oil Chemists' Society* 97, no. 7 (2020): 717–727.

35. D. Bolonio, A. Llamas, J́ Rodŕiguez-Fernández, et al., "Estimation of Cold Flow Performance and Oxidation Stability of Fatty Acid Ethyl Esters From Lipids Obtained From *Escherichia coli*," *Energy & Fuels* 29, no. 4 (2015): 2493–2502.

36. N. D. D. Carareto, C. D. Y. C. S. Kimura, E. C. Oliveira, M. C. Costa, and A. J. A. Meirelles, "Flash Points of Mixtures Containing Ethyl Esters or Ethylic Biodiesel and Ethanol," *Fuel* 96 (2012): 319–326.

37. United States Department of Agriculture, "Oilseeds: World Markets and Trade," (2025).

38. K. A. Adedokun, S. O. Imodoye, I. O. Bello, A.-A. Lanihun, and I. O. Bello, "Chapter 18—Therapeutic Potentials of Medicinal Plants and Significance of Computational Tools in Anti-Cancer Drug Discovery," in *Phytochemistry, Computational Tools and Databases in Drug Discovery*, eds. C. Egbuna, M. Rudrapal, and H. Tijjani, (Elsevier, 2023): 393–455.

39. M. Ali Ijaz Malik, S. Zeeshan, M. Khubaib, et al., "A Review of Major Trends, Opportunities, and Technical Challenges in Biodiesel Production From Waste Sources," *Energy Conversion and Management: X* 23 (2024): 100675.

40. F. Farivar, P. L. Yap, K. Hassan, et al., "Unlocking Thermogravimetric Analysis (TGA) in the Fight Against "Fake Graphene" Materials," *Carbon* 179 (2021): 505–513.

41. P.-H. Cao, C.-X. Zhang, Y.-X. Ma, et al., "Extraction of Protein From Sesame Meal: Impact of Deep Eutectic Solvents on Protein Structure and Functionality," *LWT* 187 (2023): 115366.

ijer, 2026, 1, Downloaded from https://onlinelibrary.wiley.com/doi/10.1155/er/8176983 by Hanyang University Library, Wiley Online Library on [16/11/2026]. See the Terms and Conditions (https://onlinelibrary.wiley.com/terms-and-conditions) on Wiley Online Library for rules of use; OA articles are governed by the applicable Creative Commons License

42. W.-H. Chen, Y.-S. Chu, J.-L. Liu, and J.-S. Chang, "Thermal Degradation of Carbohydrates, Proteins and Lipids in Microalgae Analyzed by Evolutionary Computation," *Energy Conversion and Management* 160 (2018): 209–219.

43. L. Hu, S. Xu, Z. Zhao, et al., "Ynamides as Racemization-Free Coupling Reagents for Amide and Peptide Synthesis," *Journal of the American Chemical Society* 138, no. 40 (2016): 13135–13138.

44. J. Berglund, T. Angles d'Ortoli, F. Vilaplana, et al., "A Molecular Dynamics Study of the Effect of Glycosidic Linkage Type in the Hemicellulose Backbone on the Molecular Chain Flexibility," *The Plant Journal* 88, no. 1 (2016): 56–70.

45. C. Wang, J. Yang, J. Wen, et al., "Structure and Distribution Changes of Eucalyptus Hemicelluloses During Hydrothermal and Alkaline Pretreatments," *International Journal of Biological Macromolecules* 133 (2019): 514–521.

46. A. Zheng, L. Jiang, Z. Zhao, et al., "Impact of Torrefaction on the Chemical Structure and Catalytic Fast Pyrolysis Behavior of Hemicellulose, Lignin, and Cellulose," *Energy & Fuels* 29, no. 12 (2015): 8027–8034.

47. G. Park, D. Choi, J. Y. Kim, S. Jung, Y. F. Tsang, and E. E. Kwon, "Direct Conversion of Cottonseeds Into Biodiesel," *Chemical Engineering Journal* 493 (2024): 152491.

48. H. Tada, M. Takamura, and M.-a. Kawashiri, "Chapter Five—Genomics of Hypertriglyceridemia," in *Advances in Clinical Chemistry*, ed. G. S. Makowski, (Elsevier, 2020): 141–169.

49. P. Kumar, et al., "Chapter 4—Hydrodeoxygenation of Triglycerides for the Production of Green Diesel: Role of Heterogeneous Catalysis," in *Hydrocarbon Biorefinery*, eds. S. K. Maity, K. Gayen, and T. K. Bhowmick, (Elsevier, 2022): 97–126.

50. H. Seifi and S. M. Sadrameli, "Bound Cleavage at Carboxyl Group-Glycerol Backbone Position in Thermal Cracking of the Triglycerides in Sunflower Oil," *Journal of Analytical and Applied Pyrolysis* 121 (2016): 1–10.

51. C. T. Alves, M. A. Peters, and J. A. Onwudili, "Application of Thermogravimetric Analysis Method for the Characterisation of Products From Triglycerides During Biodiesel Production," *Journal of Analytical and Applied Pyrolysis* 168 (2022): 105766.

52. H. Zhang, Z. Wang, and O. Liu, "Development and Validation of a GC–FID Method for Quantitative Analysis of Oleic Acid and Related Fatty Acids," *Journal of Pharmaceutical Analysis* 5, no. 4 (2015): 223–230.

53. A. Y. Widianto, J. Aubin, C. Xuereb, and M. Poux, "Gas-Liquid-Liquid Reactions: Contacting Mechanisms and Effective Process Technologies," *Catalysis Today* 346 (2020): 46–57.

54. S. Lee, M. Kim, J. Y. Kim, H. Song, I.-H. Nam, and E. E. Kwon, "Utilising Polyester and Steel Slag-Derived Metal/Carbon Composites as Catalysts in Biodiesel Production," *International Journal of Energy Research* 2024, no. 1 (2024): 1925113.

55. B. S. Sánchez, B. Benitez, C. A. Querini, and G. Mendow, "Transesterification of Sunflower Oil With Ethanol Using Sodium Ethoxide as Catalyst. Effect of the Reaction Conditions," *Fuel Processing Technology* 131 (2015): 29–35.

56. K. D. Fárníková, E. Pluhařová, A. Pysanenko, M. Fárník, Y. Yan, and J. Lengyel, "Dynamics of Collisions and Uptake of Alcohol Molecules With Hydrated Nitric Acid Clusters," *Faraday Discussions* 251, no. 0 (2024): 296–312.

57. J. Li, J. Liu, X. Sun, and Y. Liu, "The Mathematical Prediction Model for the Oxidative Stability of Vegetable Oils by the Main Fatty Acids Composition and Thermogravimetric Analysis," *LWT* 96 (2018): 51–57.

58. X. Cao, X. Luo, A. Heydari, et al., "Vortex Fluidic Mediated Generation of Fatty Acid Ethyl Esters From Vegetable Oils for Applications in Cosmetic Emulsions," *Journal of Cleaner Production* 494 (2025): 145006.

59. P. Verma and M. P. Sharma, "Comparative Analysis of Effect of Methanol and Ethanol on Karanja Biodiesel Production and Its Optimisation," *Fuel* 180 (2016): 164–174.

60. K. G. Georgogianni, M. G. Kontominas, P. J. Pomonis, D. Avlonitis, and V. Gergis, "Alkaline Conventional and in Situ Transesterification of Cottonseed Oil for the Production of Biodiesel," *Energy & Fuels* 22, no. 3 (2008): 2110–2115.

61. T. Janković, A. J. J. Straathof, I. R. McGregor, and A. A. Kiss, "Bioethanol Separation by a New Pass-Through Distillation Process," *Separation and Purification Technology* 336 (2024): 126292.

62. H. A. Saffy, W. F. Northrop, D. B. Kittelson, and A. M. Boies, "Energy, Carbon Dioxide and Water Use Implications of Hydrous Ethanol Production," *Energy Conversion and Management* 105 (2015): 900–907.

63. I. Chanakaewsomboon, C. Tongurai, S. Photaworn, S. Kungsanant, and R. Nikhom, "Investigation of Saponification Mechanisms in Biodiesel Production: Microscopic Visualization of the Effects of FFA, Water and the Amount of Alkaline Catalyst," *Journal of Environmental Chemical Engineering* 8, no. 2 (2020): 103538.

64. P. Zhang, Z. Chang, D. Wang, B. J. Blamo, and W. Li, "Effect of Water Content on Product Distribution of Base-Catalyzed Transesterification," *Waste and Biomass Valorization* 8, no. 1 (2017): 95–102.

65. A. M. M. Saeed, S. Sharma, S. Z. Hassan, A. M. Ghaleb, and G.-P. Cao, "Intensification and Optimization of FAME Synthesis via Acid-Catalyzed Esterification Using Central Composite Design (CCD)," *ACS Omega* 8, no. 29 (2023): 26206–26217.

66. L. M. Serrano-Bermúdez, C. A. Monroy-Peña, D. D. Moreno, et al., "Kinetic Model for the Esterification of Free Fatty Acids From Palm Oil With Methanol Using Sulfuric Acid as Catalyst and Sensitivity Analysis in Tubular Reactors," *Journal of the American Oil Chemists' Society* 99, no. 3 (2022): 253–263.

67. N. Narkhede, S. Singh, and A. Patel, "Recent Progress on Supported Polyoxometalates for Biodiesel Synthesis via Esterification and Transesterification," *Green Chemistry* 17, no. 1 (2015): 89–107.

68. A. S. Silitonga, H. H. Masjuki, T. M. I. Mahlia, H. C. Ong, W. T. Chong, and M. H. Boosroh, "Overview Properties of Biodiesel Diesel Blends From Edible and Non-Edible Feedstock," *Renewable and Sustainable Energy Reviews* 22 (2013): 346–360.

69. P. S. Yadav, Z. Said, R. Gautam, R. Raman, and H. Caliskan, "Novel Investigation on Atomization, Performance, and Emission Characteristics of Preheated Jatropha Oil Methyl Ester and Ethyl Ester," *Energy* 270 (2023): 126870.

70. M. Sánchez, F. Bergamin, E. Peña, M. Martínez, and J. Aracil, "A Comparative Study of the Production of Esters From Jatropha Oil Using Different Short-Chain Alcohols: Optimization and Characterization," *Fuel* 143 (2015): 183–188.

71. H. Joshi, B. R. Moser, and T. Walker, "Mixed Alkyl Esters From Cottonseed Oil: Improved Biodiesel Properties and Blends With Diesel Fuel," *Journal of the American Oil Chemists' Society* 89, no. 1 (2012): 145–153.

72. V. Kumbhar, A. Pandey, C. R. Sonawane, A. S. El-Shafay, H. Panchal, and A. J. Chamkha, "Statistical Analysis on Prediction of Biodiesel Properties From Its Fatty Acid Composition," *Case Studies in Thermal Engineering* 30 (2022): 101775.

73. W. Wang, F. Li, and Y. Li, "Effect of Biodiesel Ester Structure Optimization on Low Temperature Performance and Oxidation Stability," *Journal of Materials Research and Technology* 9, no. 3 (2020): 2727–2736.

ijer, 2026, 1, Downloaded from https://onlinelibrary.wiley.com/doi/10.1155/er/8176983 by Hanyang University Library, Wiley Online Library on [16/11/2026]. See the Terms and Conditions (https://onlinelibrary.wiley.com/terms-and-conditions) on Wiley Online Library for rules of use; OA articles are governed by the applicable Creative Commons License

74. D. Costa do Nascimento, N. D. Dorighello Carareto, A. Marinho Barbosa Neto, V. Gerbaud, and M. C. da Costa, "Flash Point Prediction With UNIFAC Type Models of Ethylic Biodiesel and Binary/Ternary Mixtures of FAEEs," *Fuel* 281 (2020): 118717.

75. A. Pumpuang, N. Klinkaew, K. Yoeng, L. Hin, A. Maneedaeng, and E. Sukjit, "The Effect of Various Feedstock Alkyl Esters on Fuel Lubrication and Properties," *Cleaner Engineering and Technology* 26 (2025): 100942.

76. D. Bolonio, M. D.-J. A. García-Martínez, M. F. Ortega, M. D. Lapuerta, J. Rodríguez-Fernández, and L. Canoira, "Fatty Acid Ethyl Esters (FAEEs) Obtained From Grapeseed Oil: A Fully Renewable Biofuel," *Renewable Energy* 132 (2019): 278–283.

77. Y. Sun, S. Ponnusamy, T. Muppaneni, et al., "Transesterification of *Camelina sativa* Oil With Supercritical Alcohol Mixtures," *Energy Conversion and Management* 101 (2015): 402–409.

78. C. P. Trentini, N. Postaue, L. Cardozo-Filho, and C. da Silva, "Waste Oil/Crambe Oil Blends for Ethyl Ester Production Under Supercritical Conditions," *The Journal of Supercritical Fluids* 163 (2020): 104889.

79. E. E. Kwon, S. Kim, Y. J. Jeon, and H. Yi, "Biodiesel Production From Sewage Sludge: New Paradigm for Mining Energy From Municipal Hazardous Material," *Environmental Science & Technology* 46, no. 18 (2012): 10222–10228.

80. E. E. Kwon, H. Yi, and Y. J. Jeon, "Mechanistic Investigation Into Water Tolerance of Non-Catalytic Biodiesel Conversion," *Applied Energy* 112 (2013): 388–392.

81. S. F. Interlenghi, P. de Almeida Bruno, O. Q. F. Araujo, and J. L. de Medeiros, "Social and Environmental Impacts of Replacing Transesterification Agent in Soybean Biodiesel Production: Multi-Criteria and Principal Component Analyses," *Journal of Cleaner Production* 168 (2017): 149–162.

Supporting Information

Additional supporting information can be found online in the Supporting Information section. **Supporting Information.** Tables S1–S2: Detailed information on the GC/FID and GC/MS analytical systems, respectively. Tables S3–S4: Calibration data for FAME and FAEE standards used for GC/FID quantification, respectively. Tables S5–S6: Calibration parameters used for quantitative analysis of FAMEs and FAEEs by GC/FID, respectively. Table S7: Parameters used in the Peng–Robinson equation and estimated autogenous pressures under different reaction conditions. Table S8: Experimental data supporting Figure 3, including mean FAEE yields, standard deviations, and FAEE compositions at different reaction temperatures. Table S9: Experimental data supporting Figure 5, including mean FAEE yields, standard deviations, and FAEE compositions under varying water contents and FFA additions. Tables S10–S11: Input parameters used to predict the fuel properties of FAMEs and FAEEs, respectively. Tables S12–S13: Analysis of variance (ANOVA) results for FAEE yields obtained under different water contents and FFA additions, respectively. Table S14: Input parameters used to calculate CO_2 mitigation. Figure S1: Reactor temperature profile and time-dependent FAEE yield during thermally induced noncatalytic transesterification. Figure S2: Proposed reaction mechanism of thermally induced noncatalytic transesterification. Figure S3: Effect of the ethanol-to-oil molar ratio on FAEE yield during thermally induced noncatalytic transesterification of cottonseed oil. Figure S4: GC/MS chromatogram and identified compounds obtained from noncatalytic transesterification of cottonseed oil with ethanol at 380°C. Equations S1–S2: Equations used to estimate CO_2 mitigation through diesel substitution with biodiesel and alcohol production, respectively.

ijer, 2026, 1, Downloaded from https://onlinelibrary.wiley.com/doi/10.1155/er/8176983 by Hanyang University Library, Wiley Online Library on [16/11/2026]. See the Terms and Conditions (https://onlinelibrary.wiley.com/terms-and-conditions) on Wiley Online Library for rules of use; OA articles are governed by the applicable Creative Commons License